TABLE OF CONTENTS

CHAPTER		PAGE	
I.	INTRODUCTION	1	1/A8
II.	GENERAL INTERPRETATION	10	1/B5
III.	VALLEY FLOW	23	1/C7
	Theory of Valley Flows	23	1/C7
	Data Analysis	32	1/D8
IV.	CONCLUSIONS	52	1/F8
BIBLIOGRAPHY	. . . . .	53	1/F9

APR 3 0 1981

Item 530-H-14

NAS 1.26:3401

NASA Contractor Report 3401

ORIGINAL

COMPLETED

Analysis of the Inversion Monitoring Capabilities of a Monostatic Acoustic Radar in Complex Terrain

David Koepf and Walter Frost

CONTRACT NAS8-32031
APRIL 1981

NASA

(10)

NASA Contractor Report 3401

Analysis of the Inversion Monitoring Capabilities of a Monostatic Acoustic Radar in Complex Terrain

David Koepf and Walter Frost
The University of Tennessee Space Institute
Tullahoma, Tennessee

Prepared for
Marshall Space Flight Center
under Contract NAS8-32031

National Aeronautics
and Space Administration

Scientific and Technical
Information Branch

1981

I

AUTHORS' ACKNOWLEDGMENTS

This research was supported under NASA Contract No. NAS8-32031. The authors are grateful for the support of A. Richard Tobiason of the Office of Aeronautical and Space Technology, NASA Headquarters, Washington, D.C. Special thanks go to O. H. Vaughan and Dennis W. Camp of the Atmospheric Sciences Division, NASA/George C. Marshall Space Flight Center, Alabama, for their direct support of the research program.

The authors also thank Dr. James Connell for his guidance in the development of this research program and Henry Leckenby and other TVA personnel responsible for the data acquisition and reduction. The authors also thank Judy Wright and Barbara Smith for typing the final draft and Robert Suttles for aid in preparation of the figures.

ABSTRACT

A qualitative interpretation of the records from a monostatic acoustic radar is presented. This is achieved with the aid of airplane, helicopter, and rawinsonde temperature soundings. The diurnal structure of a mountain-valley circulation pattern is studied with the use of two acoustic radars, one located in the valley and one on the downwind ridge. The monostatic acoustic radar was found to be sufficiently accurate in locating the heights of the inversions and the mixed layer depth to warrant use by industry even in complex terrain.

TABLE OF CONTENTS

CHAPTER		PAGE
I.	INTRODUCTION	1
II.	GENERAL INTERPRETATION	10
III.	VALLEY FLOW	23
	Theory of Valley Flows	23
	Data Analysis	32
IV.	CONCLUSIONS	52
BIBLIOGRAPHY		53

LIST OF FIGURES

FIGURE		PAGE
1.	Three Possible Configurations Used in Atmospheric Acoustic Sounding	4
2.	Map of Widows Creek Steam Plant	5
3.	Acoustic Records for Widows Creek Steam Plant (Valley Location)	14
4.	Acoustic Records for The University of Tennessee Space Institute, June 3-4, 1978	19
5.	Simplified Circulation Pattern of the Valley-Plain Breeze	24
6.	Valley-Plain Breeze Illustrating the Counter Current Aloft	26
7.	Hourly Averaged Wind Roses (Wind Directional Percentages) August 1978	27
8.	Arbitrary Wind Profiles Illustrating the Low Level Jet	33
9.	Acoustic Records for Widows Creek Steam Plant (Parallel Operation, Valley Location), October 1-2, 1978	35
10.	Acoustic Records for Widows Creek Steam Plant (Parallel Operation, Valley Location), October 3-4, 1978	36
11.	Acoustic Records for Widows Creek Steam Plant (Parallel Operation, Valley Location), October 4-5, 1978	37
12.	Acoustic Records for Widows Creek Steam Plant, October 11-12, 1978	41
13.	Acoustic Records for Widows Creek Steam Plant, October 21-22, 1978	43
14.	Acoustic Records for Widows Creek Steam Plant, October 23-24, 1978	46

CHAPTER I

INTRODUCTION

An investigation of the inversion monitoring capabilities of a monostatic acoustic radar is presented. This is accomplished simultaneously with an investigation of inversion behavior in the vicinity of a deep river valley. The monostatic acoustic radar is analyzed with regard to noise and accuracy in locating and monitoring inversions. The behavior of inversions, the number, and heights of formation and breakup are investigated with respect to the complex valley climatology and flow phenomenon.

Acoustic radars promise to provide an economical method of monitoring the structure of the planetary boundary layer. Conventional rawinsonde methods of monitoring the atmosphere are expensive and, therefore, they are traditionally used only a few times daily. The cost of aircraft soundings in the atmosphere is even more prohibitive than that of rawinsonde. Acoustic radars can provide continuous monitoring of the atmosphere as compared to periodic aircraft or rawinsonde flights.

Continuous monitoring of the planetary boundary layer is helpful in maintaining both air quality and air safety standards. This study was conducted to assess the usefulness of an acoustic radar for continuous monitoring of climatological factors, particularly inversion layers which influence the dispersion of pollutants in the atmosphere.

The acoustic radar is an active remote sensing device. A sound wave is transmitted either vertically or at a given angle into the atmosphere. The sound waves are scattered, reflected, and Doppler shifted

by density inhomogeneities and wind shears within the atmosphere. These inaudible echoes can be received and processed according to the specific needs of the user.

Sonar was one of the first active acoustic sounders. Both the Navy and the fishing industry found sonar to be an invaluable tool. Seismologists have used passive and active acoustic devices for many years. Exploding rockets were used for the first high altitude temperature estimates, but it was not until 1968 when McAllister [1][1] developed what he preferred to call the "echosonde" that atmosphere scientists began to realize some of the potential of using sound as a remote sensing tool.

Acoustic techniques can provide vertical soundings up to 1.5 km altitude. From the echoes received, the three-dimensional wind field, inversion strength, and the three-dimensional spectral density functions for temperature and wind velocity can be estimated with time resolution better than five minutes, i.e., almost continuously [2].

There are a number of acoustic radar configurations used in boundary layer sounding. The monostatic mode refers to a collocated transmitter-receiver and receives only the backscattered echoes [1]. In this mode the three-dimensional spectral density function for temperature fluctuations, the heights and strengths of inversions, and often the height of the mixed layer can be estimated. By separating the transmitter from the receiver, the three-dimensional spectral density

---

[1]Numbers in brackets refer to similarly numbered references in the Bibliography.

function for velocity fluctuations can also be estimated. This configuration is referred to as the bistatic mode and can be combined with a monostatic unit for little additional cost. Placing a third transmitter perpendicular to the other two allows one to measure the three orthogonal components of the wind. This is achieved by measuring the Doppler shift in frequency caused by the movement of the scattering element and, therefore, this mode of operation is referred to as Doppler acoustic radar. These three modes of operation are shown in Figure 1.

Experimental Applications of an Acoustic Radar

The Aerovironment[2] model 300 monostatic-bistatic acoustic radar was operated as continuously as possible from the spring of 1977 until the summer of 1978 by The University of Tennessee Space Institute (UTSI). This was first used in an advection fog research program funded under NASA contract NAS8-32031. The unit was operated in both monostatic and bistatic modes in conjunction with standard meteorological towers and a tethered balloon for vertical profiles of temperature, humidity, wind speed and direction. One individual run during that study is presented in Chapter II, page 19, to illustrate a cause of noise.

A joint study with the Tennessee Valley Authority (TVA) was carried out following the fog study. Two identical acoustic radars were operated near the Widows Creek Steam Plant along the Tennessee River at Stevenson, Alabama. Figure 2 is a map of the steam plant and the surrounding area. TVA operates an air quality program which involves

[2]Trade name for Aerovironment, Inc., Pasadena, California.

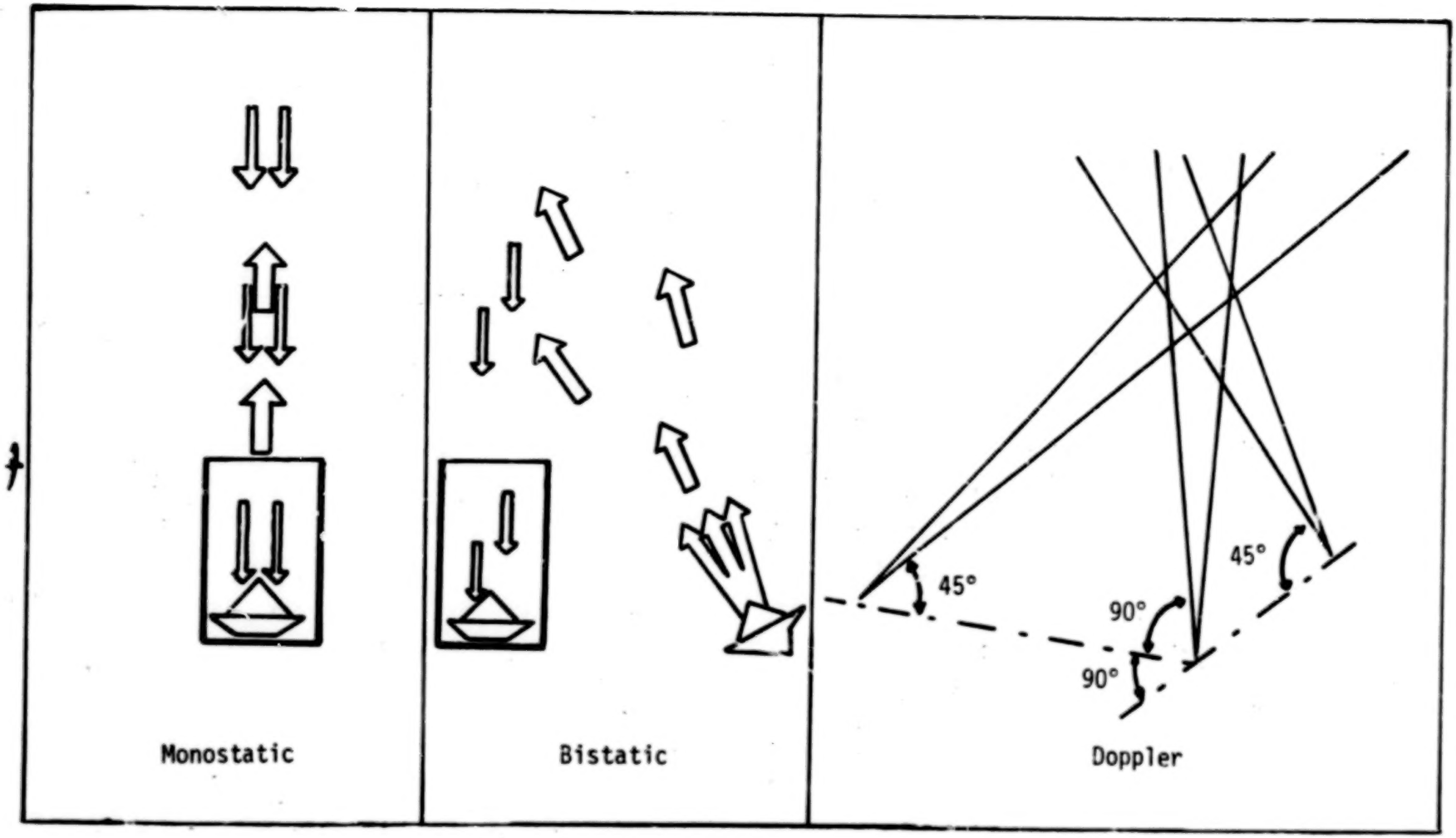

Figure 1. Three possible configurations used in atmospheric acoustic sounding.

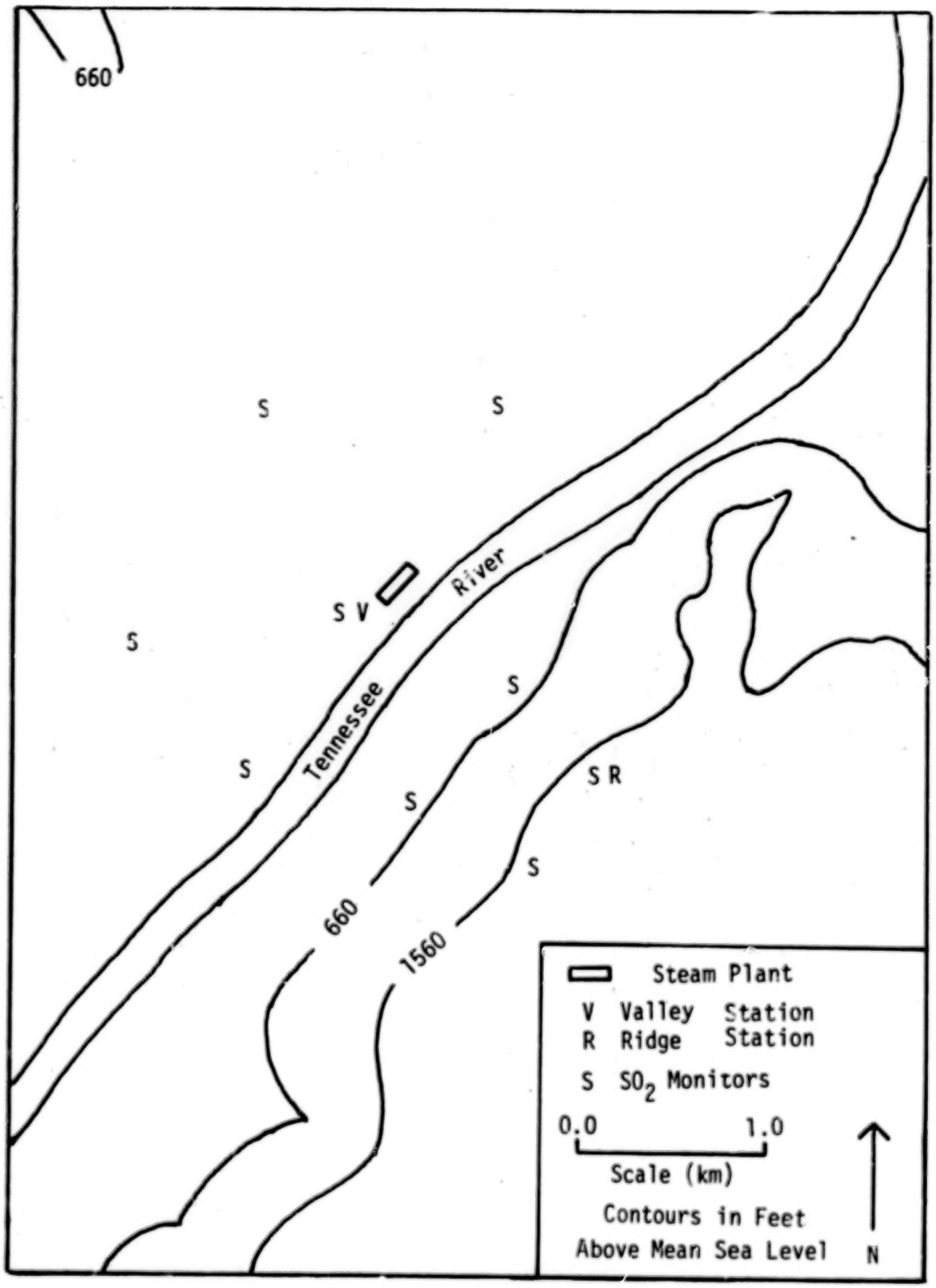

Figure 2. Map of Widows Creek steam plant.

two mesoscale weather stations, one in the valley and one near the edge of the downwind ridge. Temperature soundings were made periodically by rawinsonde, helicopter, and airplane flights. The instruments used in this study are listed in Table 1. In addition to the instruments listed in Table 1, hourly observations of sky cover and plume condition were made by TVA employees. All data for wind speed and direction, temperature, insolation, pressure and SO_2 concentration were reduced by TVA and provided to UTSI in tabular form.

Data Acquisition

Mean wind speed and direction were measured by TVA's two 61-meter towers at 10 and 61 meters. The data were averaged for one-hour periods and supplied in tabular form. Insolation was measured at the valley meteorological station, indicated by a "V" in Figure 2, by a pyrheliometer. Hourly readings were supplied. Pilot balloons were launched from the valley meteorological station approximately every one to two hours (weather permitting) and tracked by single theodolite to estimate the wind field.

Temperature soundings were made by aircraft following approximately a 1-mile diameter spiral up to 1.5 kilometers. When atmospheric conditions prohibited aircraft flights, rawinsonde measurements were taken. Rawinsonde packages were released from the valley location. Calibration of aircraft temperature measurements was accomplished by flying as close as possible to the 61-meter tower located at the valley meteorological station and adjusting the aircraft temperature reading to that of the temperature indicated at 61 meters by the tower

TABLE 1

TVA WIDOWS CREEK AIR QUALITY MONITORING INSTRUMENTATION AND SETUP

Instrument	Time	Location	Desired Quantity
Two monostatic acoustic radars	Continuous	Valley, ridge	Inversions
Two 61-meter towers instrumented at 61 and 10 meters	Continuous	Valley, ridge	Three-dimensional wind field
Pyrheliometer	Continuous	Valley	Insolation
Pibal	Periodic	Valley	Three-dimensional wind field
Rawinsonde	Periodic	Valley	Three-dimensional wind field and lapse rate
Airplane or helicopter flights	Periodic	Valley	Lapse rate
Microbarograph	Continuous	Valley	Pressure and pressure tendency
SO_2 monitors	Continuous	Surrounding Area	SO_2 concentration

instrumentation. All temperature soundings in this study are from air-plane flights unless otherwise specified.

A microbarograph located at the valley meteorological station was used to determine atmospheric pressure. Hourly readings were supplied.

Electrochemical SO_2 monitors were located in a spherical pattern surrounding the Widows Creek Steam Plant in the valley and on the downwind ridge. The locations of the monitors are shown in Figure 2. Hourly SO_2 concentrations were provided if the concentration exceeded 0.01 parts per million.

The University of Tennessee operated two identical acoustic radars, one of which is owned by NASA and the other by TVA. TVA supplied the support data from the aforementioned instruments used in this study.

The investigation consists of two parts. During the first part of the study, both acoustic radars were operated side by side at the valley meteorological station. This was done to test the height and time scales of one radar against the other and also allowed for some adjustment in the sensitivity of the two radars. The adjustment, however, was not totally satisfactory due to the difference in physical conditions of the two identical radars.

The second part of the investigation was designed to monitor the behavior of inversions within the valley as compared to that on the downwind ridge. One acoustic radar was moved up to TVA's air quality monitoring station on the southeast ridge. The other was left in the valley. The difference in heights and durations of inversions inside

and outside of the valley is studied. This is done with respect to the valley flow phenomenon.

A brief description of the theory and assumptions used in acoustic sounding is presented in Chapter II. A general interpretation of the major features on four acoustic records is presented. A description and analysis of noise sources in acoustic sounding are also included in Chapter II.

Chapter III consists of two parts. The first section gives an introduction to the theory involved concerning the valley flow phenomenon. Meteorological wind roses for August from the Tennessee River Valley illustrate the valley flow phenomenon and are presented in this section. Section 2 consists of the major analysis of the acoustic records taken during this study. The acoustic records are analyzed for inversion heights and durations and are compared with the synoptic and mesoscale weather phenomena as indicated by the supporting climatological data.

CHAPTER II

GENERAL INTERPRETATION

Theory

To better understand the concept of an acoustic radar, a brief explanation of the theory and assumptions is presented in this section. A full derivation of wave propagation is not presented, however, and the reader is referred to Monin [3] or Tatarski [4] for this information.

As is the case with all radars, waves are transmitted, reflected, and received by the radar. The strength and location of the echo is then recorded in a convenient format. With conventional radars the desired echo producers are solid objects such as raindrops or some other form of tracer. Although the acoustic radar "sees" these solid objects, they are not the desired echo producers and appear as noise on the record. The acoustic radar is designed to record the extremely weak echoes from temperature variations or other inhomogeneities in clear air.

If the atmosphere were totally still and homogeneous, sound waves would satisfy the homogeneous wave equation,

$$\nabla^2 p + k^2 p = 0 \qquad (1)$$

where p is the pressure and k is the wave number.

In a nonhomogeneous atmosphere there is always some scattering of sound waves. Separating the wave into an incident and a scattered wave and neglecting the higher order terms results in the scattering equation

$$\nabla^2 p + k^2 p = 2k^2 n' p \qquad (2)$$

The quantity of interest here is n', which is the fluctuating refractive index for sound in the nonhomogeneous atmosphere. This equation, also known as the Born approximation to the acoustic wave equation, is a second-order approximation and any errors introduced can be reasonably neglected.

In order to relate the reflected acoustic power to transmitted acoustic power, a scattering cross section is defined as the ratio of scattered flux density to transmitted flux density per unit solid angle, per unit thickness of the scattering element.

$$\sigma(\theta) \equiv \frac{\langle s \rangle r^2}{S_o V} \tag{3}$$

Here s and S_o are the acoustic energy flux densities of the scattered and initial sound pulse, respectively. Theta is the angle formed between the initial and scattered waves. The brackets denote an ensemble average and r is the distance from the transmitter to the scattering volume, V.

The turbulence in the scattering volume is assumed to be analogous to diffraction gratings with a spacing equivalent to the characteristic length of the turbulent motion, ℓ, and with a cross-sectional area equal to the scattering cross section.

$$\ell = \frac{\lambda}{2\left|\sin\left(\frac{\theta}{2}\right)\right|} \tag{4}$$

Equation 4 is known as the Bragg condition and gives the angle θ for the principal maxima in the diffraction pattern created by passing waves of length λ through a diffraction grating of spacing ℓ.

For homogeneous isotropic turbulence, Tatarski [5], using the above assumptions, arrived at what is used today for the scattering cross section in the acoustic radar equation

$$\sigma(\theta) = \frac{\pi}{2} k^4 \cos^2\theta \left(\frac{\phi_T K}{T_0^2} + \frac{E(K) \cos^2\left(\frac{\theta}{2}\right)}{c} \right) \tag{5}$$

Here $K = 2k \sin\left(\frac{\theta}{2}\right)$ is the turbulence wave number and ϕ_T and $E(K)$ are the three-dimensional spectral density functions for temperature and wind velocity fluctuations, respectively. T_0 is an appropriate average temperature which will influence both terms of the equation since c, the velocity of sound, is also a function of temperature.

In the Kolmogorov inertial subrange, Equation 5 reduces to

$$\sigma(\theta) = 0.03k^{1/3} \cos^2(\theta) \left(0.13 \frac{C_T^2}{T_0^2} + \frac{C_V^2}{c^2} \cos^2\left(\frac{\theta}{2}\right) \right) \left(\sin \frac{\theta}{2} \right)^{-11/3} \tag{6}$$

C_T and C_V are the structure coefficients for temperature and wind velocity, respectively. The defining equation for the temperature structure coefficient is:

$$C_T^2 = \left(\frac{T(x) - T(x - \ell)}{\ell^{2/3}} \right)^2 \tag{7}$$

Although Equation 7 is strictly valid for potential temperatures, no measurable error is introduced by using actual temperature differences.

It should be noted that for monostatic operation, $\theta = 180°$, Equation 7 reduces to a linear function of C_T^2.

$$\sigma(180) = 3.9 \times 10^{-3} \frac{C_T^2}{T_0^2} \qquad (8)$$

Analysis

Theory predicts that in the monostatic mode with the attenuation of sound being taken into account, the returned echo strength is directly proportional to the structure coefficient for temperature. Any sharp temperature discontinuity will therefore produce an echo. Although sharp density gradients do not exist for any length of time in the atmosphere, turbulence along even a weak discontinuity continuously sets up and breaks down strong gradients. The result is that even weak inversions produce echoes if sufficient turbulence exists along the boundary.

A comparison of the heights of inversions as indicated by aircraft and monostatic acoustic radar for the period October 25 to October 28, 1978, is presented in this section. The acoustic record shows that the acoustic radar is as accurate as aircraft temperature soundings in locating the inversion heights.

Figure 3 shows the acoustic records for the period October 25-26, 26-27, and 27-28, 1978, produced by TVA's acoustic radar located at the valley meteorological station.

The chart records are for a 24-hour period beginning at 1700 LST (local standard time). The time of 1700 LST was chosen because of the obvious change in atmosphere structure which usually occurs between 1600 and 1800 LST. The decay of daytime thermals and formation of nocturnal inversions usually occurs during this period.

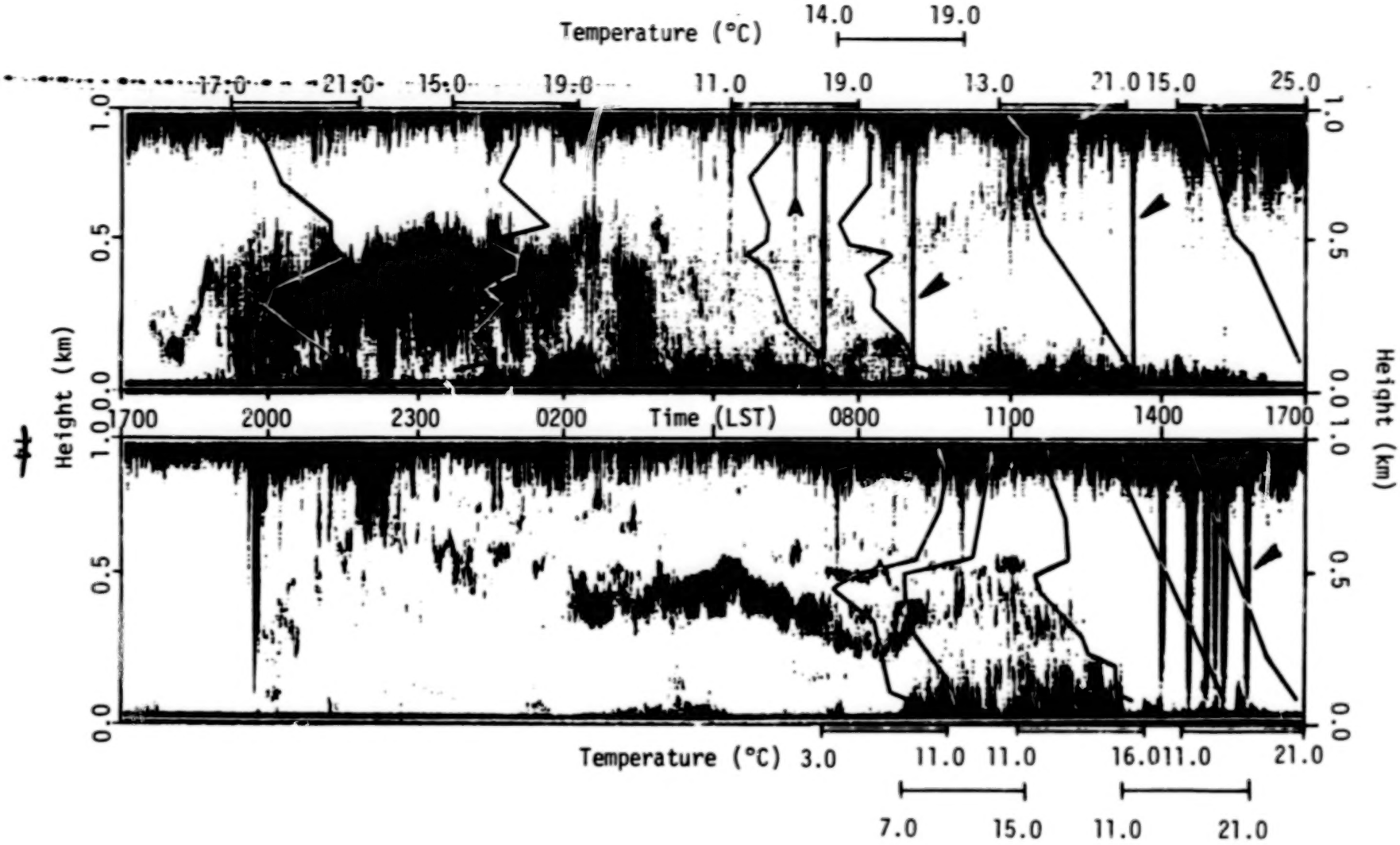

Figure 3. Acoustic records for Widows Creek steam plant (valley location).
(a) October 25-26, 1978 (upper chart) (b) October 26-27, 1978 (lower chart).
Symbols ◄ and A: Non-atmospheric noise.

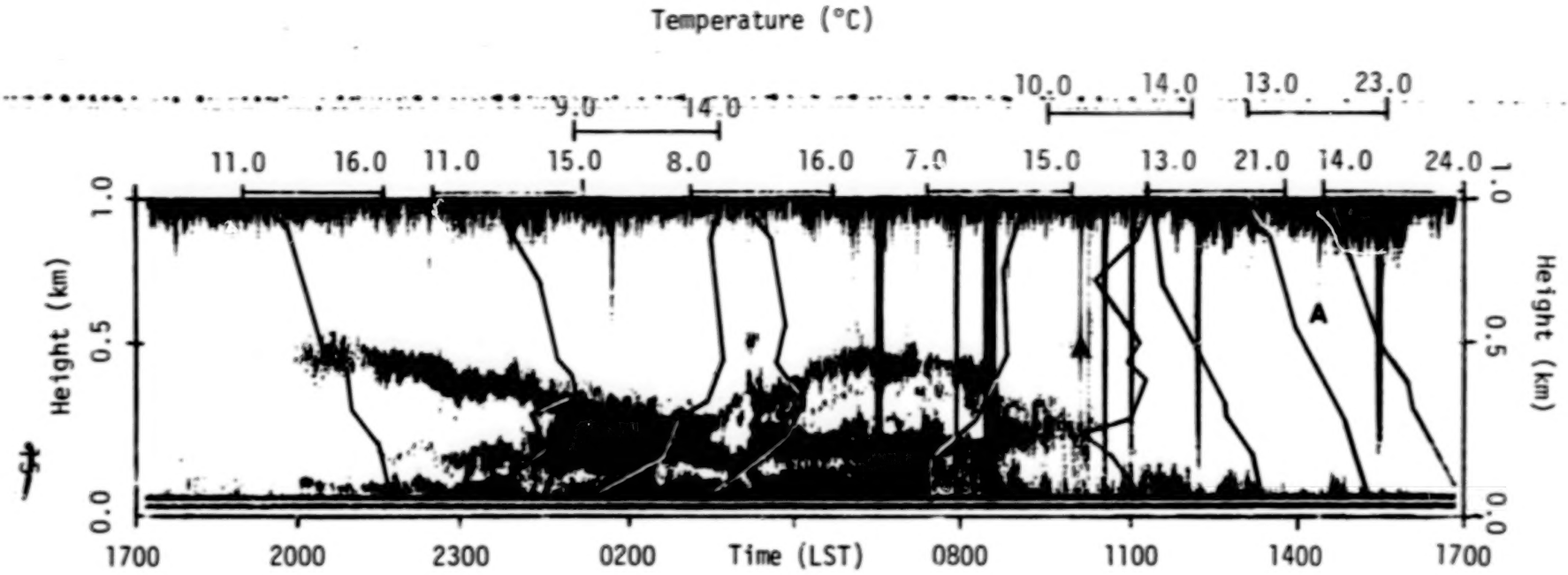

Figure 3. (continued). (c) October 27-28, 1978.

Six airplane temperature soundings were made during the time period shown in Figure 3(a), five for 3(b), and nine for 3(c). Temperature profiles from these soundings are overlaid (the same height scale) on the acoustic records at the appropriate time. The temperature profiles were drawn by a computer graphics program which determines the scale of each individual case based on the data. The temperature scales therefore are not always identical. The temperature scale is indicated directly above or below each profile. There is almost perfect agreement in the heights of the inversions indicated by the acoustic radar and the temperature soundings. No quantitative comparison is attempted with regard to the strength of the inversions because the acoustic radar calibration is not known. The sensitivity was set only to produce a meaningful qualitative record. The aircraft was not equipped to measure turbulence and therefore values of C_T could not be calculated and the acoustic radar's calibration could not be tested.

Three common types of inversions that occurred in the Tennessee Valley during this study are shown in Figure 3. Figure 3(a) illustrates a nocturnal ground-based inversion which elevates and separates from the surface. Figure 3(b) illustrates a typical formation, strengthening, and decay of an elevated nocturnal inversion. Figure 3(c) shows an elevated nocturnal inversion lowering to meet a deepening ground-based inversion. Both inversions then leave the surface, separate and eventually decay by 1000 LST.

During late evening on October 26, left side of Figure 3(b), the formation of an inversion between 300 and 600 meters is apparent. Rawinsonde measurements at 2107 LST indicate that the base of the

inversion occurred at 450 meters with an approximately isothermal layer above for 300 meters. This was a thick, but weak, inversion layer. The acoustic radar shows a very disorganized inversion layer since a sharp gradient or strong turbulence across a weak gradient is necessary to produce an echo. It is likely that the turbulence was insufficient across the inversion during this "quiet" period to show the weak inversion observed from the rawinsonde measurements.

Noise

Noise is defined differently according to specific needs. The major characteristic in most definitions is: that which is unwanted or distorted. Therefore, noise is referred to herein as undesirable sources of sound which either distort or place spurious signals on the acoustic radar record.

Since the desired return echo of an acoustic radar has extremely low power levels, there are many sources of noise which affect acoustic soundings. These sources of noise are classified for purposes of the following discussion into two categories based on origin--atmospheric and non-atmospheric.

Major non-atmospheric sources of noise are those which radiate sound of wavelength within the band-pass range of the acoustic radar. Such sources are cars, lawn mowers, electric fans, etc., which all produce noise on the record. Large lead shields padded with foam are used to eliminate these sources of noise. However, they cannot all be eliminated; the dark vertical lines spanning the chart record, for example, are a result of these types of noise sources. Figure 3

and Figure 4 show a number of these lines, a few of which are indicated by an arrow.

Other sources of non-atmospheric noises are electron shot noise, unsatisfactory line current and other system problems inherent in facsimile recorders. Electron shot noise is easily calculated and is found to be negligible compared to the level of the desired signal and other noise sources. The incoming ac line current creates a problem that can be recognized by the operator. Although not occurring in the records of this study, an unuseable signal results when a 110-volt square wave input from a 12-volt inverter is used to power the acoustic radar. One of the largest sources of noise is inherent to the facsimile recorder itself. In theory, facsimile recorders should be nearly noise-free. In practice, however, they scrape, burn, and tear the recording paper. The pen and conductive plate must be cleaned on at least a weekly basis to insure proper operation. These sources of noise can, with proper maintenance and operation procedures, be eliminated or accounted for when interpreting the recorded data.

A third major source of non-atmospheric noise results from solid objects which pass through the scattering volume or through a side lobe of the antenna pattern. Airplanes, flocks of birds, and helicopters are common examples. Echoes from airplanes appear as thin vertical lines on the record. A number of these lines appear on Figures 3 and 4, a few of which are indicated on the chart by an "A." Nearby trees and buildings appear as horizontal lines on the record. Thus, they also are non-atmospheric sources of noise. Figure 4 shows the effect of a single building located 300 meters from the radar. Note the horizontal line

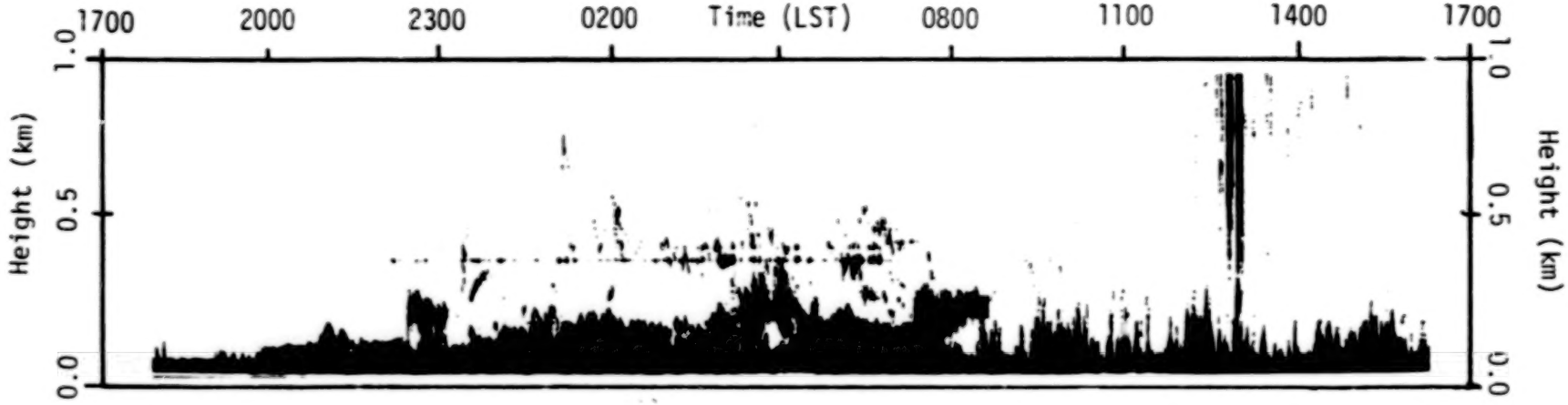

Figure 4. Acoustic records for The University of Tennessee Space Institute, June 3-4, 1978.

(Horizontal line is reflection from building.)

at approximately 400 m during the period from 2000 LST until 0900 LST. The echo from another building appears later in the evening (2400 LST) slightly above the first. Echoes from buildings generally appear only at night when the humidity is high and the atmosphere is stable. These nocturnal conditions produce higher refractive bending of the sound waves and a side lobe of the antenna reflected off the buildings. The height of the echo on the chart is approximately the distance from the antenna to the building. This source of noise is easily recognized and can be taken care of by moving the antenna.

There are three sources of atmospheric noise that are significant to this study--rain, wind, and thermal noise. Rain will totally blacken the chart. The desired signal is too weak to be recorded over the sound of rain on the antenna.

Wind noise appears as a shading on the chart from light gray at the bottom to black at the top. The change in the intensity of this noise with height is due to the nonlinear amplification designed into the recorder. This design feature accounts for the loss in acoustic power due to atmospheric attenuation. No clear example of wind noise is available from this study; however, there is little doubt that wind noise appears to some degree on all of the records presented. Wind and rain noise can totally obliterate the record, and there appears no way of eliminating this noise at the present time.

Thermal noise due to the collision of air molecules with the receiver is of the same magnitude as electron shot noise and is therefore negligible.

Calibration and Presentation

Facsimile recorders can condense huge amounts of data into a concise readable format for the trained eye. The human eye, however, is a poor density discriminator, making quantitative interpretation from visual inspection difficult. Facsimile recorders are difficult to reproduce satisfactorily and, thus, considerable record content is lost in presenting the recorded data. Facsimile recorders, however, are economical and record a large amount of data. Digital techniques are now producing computer printouts which can be quantitatively analyzed, while color slicing provides significantly more readable records. The digital techniques also allow for some noise elimination and boundary enhancing. With digital systems, the Doppler shift may also be determined. The choice of system depends on the needs of the user. Digital systems are more expensive but allow for much more data to be analyzed.

Calibration of an acoustic radar is a problem equally as difficult as data recording. Calibration with tower data and airplane flights has been attempted by others, but has not, however, produced totally satisfactory results [6]. The acoustic radar measures vertical profiles of C_T^2; thus, calibration requires measuring both vertical profiles of temperature and the turbulence parameters. The latter requires the use of an inertial platform. Since the expense of aircraft so equipped is high, no known attempt has been made. It appears a Lidar system might prove more useful for calibration of the acoustic radar since both measure fluctuating refractive indices continuously.

The data analysis presented in Chapter III is therefore, for the most part, a qualitative comparison. Calibration, by placing two identical acoustic radars near each other and operating them for a month to calibrate one against the other, was attempted. The sensitivities were adjusted as accurately as possible to produce identical records. Although the acoustic radars were the same model, they were not in the same physical condition and apparently for this reason could not be adjusted to give equal intensities. Thus, quantitative measurements of temperature discontinuities were not possible. The locations of temperature inversion, however, which are not dependent on the intensity of the record, correlate very well with each other and with aircraft data. Thus, as will be shown in Chapter III, the height as well as the growth and decay patterns of inversion can be adequately monitored with an acoustic radar.

CHAPTER III

VALLEY FLOW

I. THEORY OF VALLEY FLOWS

The phenomenon of katabatic and valley winds has been observed for a long time. Besides meteorologists, however, only the people who live or work in a large mountain-valley-plain location are familiar with the valley-plain breeze. The cause, differential terrain heating and cooling due to surface orientation, is only partly understood.

The need for a heat sink by conventional electric power generating stations has traditionally limited their construction to large water bodies and river valleys. The result is that the plume trajectory is a complex diurnal function of topography and synoptic condition. This has frustrated the power companies and other industrial companies using the atmosphere as a sink for their effluent, as well as the people living in the valley.

An initial theoretical explanation of valley flow is accredited to Prandtl [7] and Defant [8]. Their classical description is illustrated schematically in Figure 5. This is clearly an over-simplified view of the circulation pattern. The slope of the valley floor, the slope of the valley walls, the prevailing wind direction, and the orientation of the valley all have dramatic effects on this pattern. A west-facing slope will experience up-slope winds after they have ceased on the east-facing slope. A crosswind will produce eddies on the lee slope and cause up-slope winds on the windward slope. Valley axis winds hamper and disguise the circulation pattern, or may even destroy it completely.

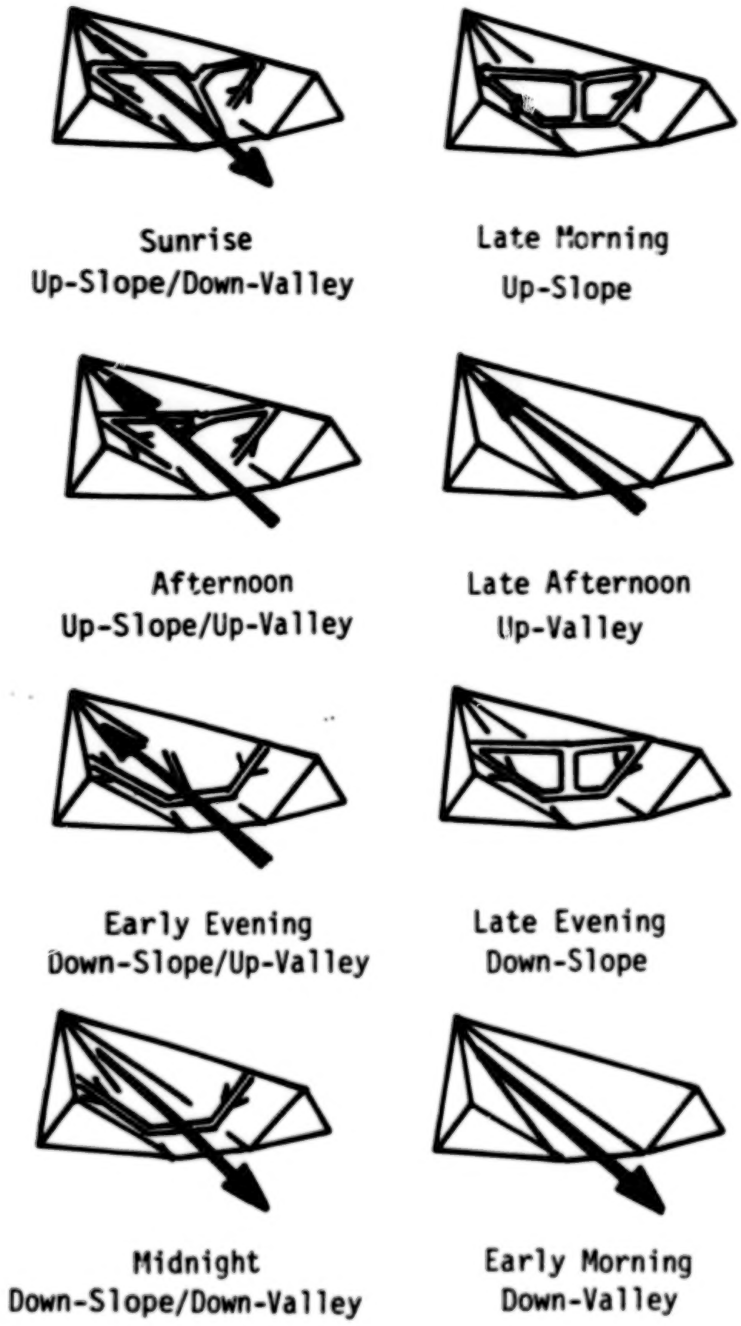

Figure 5. Simplified circulation pattern of the valley-plain breeze.

Differential heating and cooling is the cause for both land-sea and valley-plain circulation patterns. The amplitude of the diurnal temperature variation is greater in the valley than over the plain which the valley empties into or the plateau which it cuts through. The result of this temperature variation is a diurnally alternating pressure gradient which produces the up-slope/up-valley winds during the day and the down-slope/down-valley winds at night.

As with all standing circulation patterns, there must be a counter circulation pattern nearby to sustain the circulation. In the case of the valley-plain breeze there is a counter current aloft forming just above ridge height. This counter current is illustrated in Figure 6. The counter current is weaker and less frequent due to the stronger prevailing wind speeds at these heights. It seems reasonable to assume that the return circulation is often just a variation in the prevailing wind field and may not be immediately apparent. The prevailing winds, unless orientated along the valley, are much weaker in the valley; therefore, the valley-plain breeze appears much stronger and more frequent than its counterpart.

To investigate the valley-plain winds measured in this study, a computer program was written to compute wind roses using data from the two TVA 61-meter towers. One tower is located in the valley and one on the ridge. The horizontal wind field and temperature were measured at 10 m and 61 m levels for both locations. The length of a line on a wind rose is proportional to the percentage of time the wind blows from that direction. Figure 7 shows hourly averaged wind roses for the four locations for the month of August 1978. These are standard

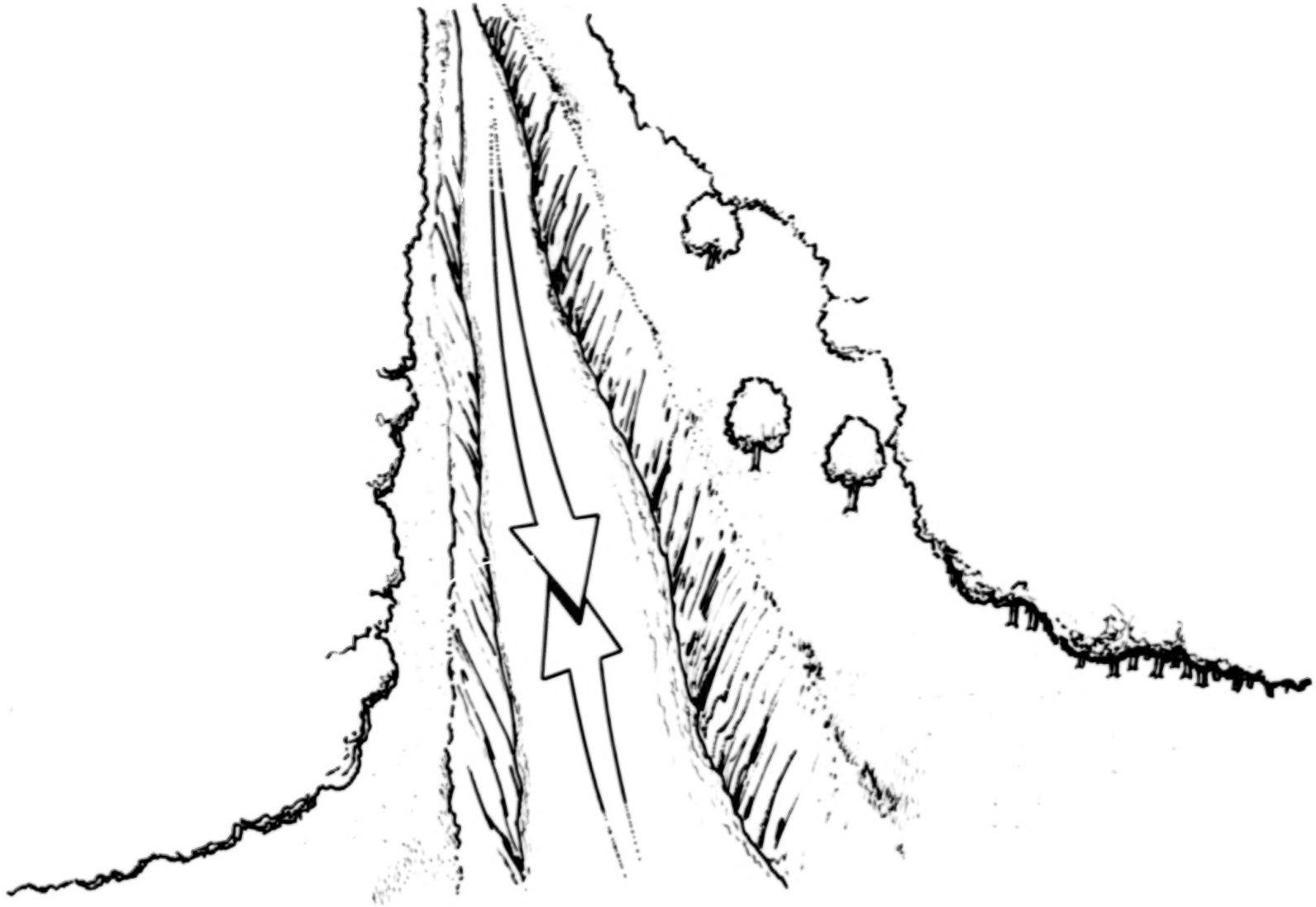

Figure 6. Valley-plain breeze illustrating the counter current aloft.

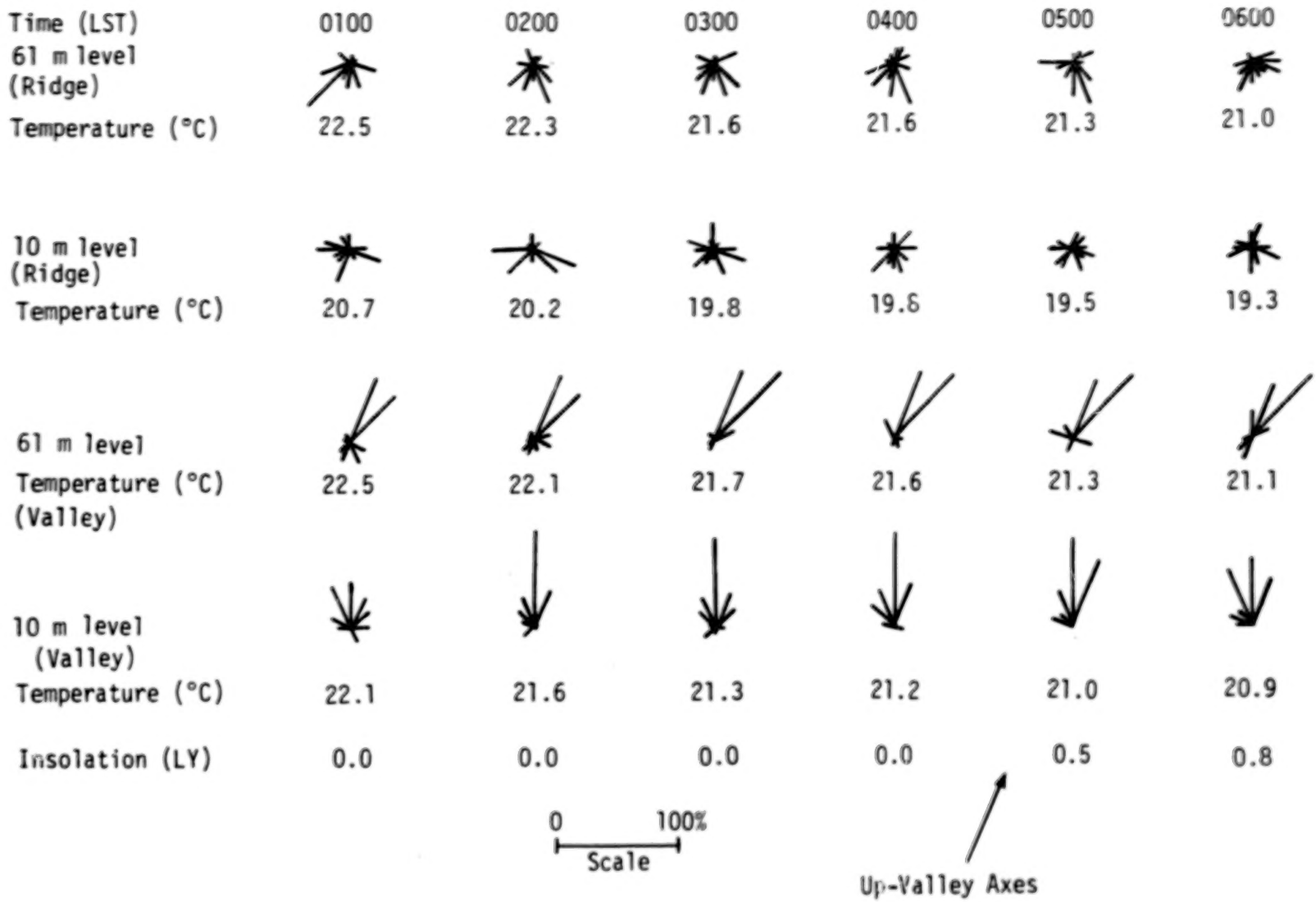

Figure 7. Hourly averaged wind roses (wind directional percentages) August 1978.

BLANK PAGE

BLANK PAGE

Time (LST)	0700	0800	0900	1000	1100	1200
61 m level						
Temperature (°C) (Ridge)	21.2	21.6	22.4	23.6	24.3	25.1
10 m level (Ridge)						
Temperature (°C)	20.0	21.9	22.9	24.3	25.1	25.9
61 m level (Valley)						
Temperature (°C)	21.1	21.6	22.6	24.4	25.8	25.9
10 m level (Valley)						
Temperature (°C)	21.2	22.1	23.3	25.2	26.7	28.0
Insolation (LY)	0.05	0.24	0.46	0.72	0.93	1.05

Figure 7. (continued).

Time (LST)	1300	1400	1500	1600	1700	1800
61 m level (Ridge)						
Temperature (°C)	26.0	26.5	26.9	26.8	26.6	26.0
10 m level (Ridge)						
Temperature (°C)	26.7	27.4	27.6	27.7	27.0	27.3
61 m level (Valley)						
Temperature (°C)	27.9	28.6	28.7	28.6	28.3	27.5
10 m level (Valley)						
Temperature (°C)	28.7	29.5	29.5	29.1	28.7	27.7
Insolation (LY)	1.05	1.05	0.88	0.65	0.45	0.22

Figure 7. (continued).

Time (LST)	1900	2000	2100	2200	2300	2400
61 m level (Ridge)						
Temperature (°C)	24.9	24.4	24.2	23.7	23.3	23.1
10 m level (Ridge)						
Temperature (°C)	24.4	22.7	22.6	21.9	21.3	21.0
61 m level (Valley)						
Temperature (°C)	27.0	26.4	25.1	24.4	23.7	23.0
10 m level (Valley)						
Temperature (°C)	26.7	25.2	24.4	23.6	23.0	22.5
Insolation (LY)	0.05	0.00	0.00	0.00	0.00	0.00

Figure 7. (concluded).

meteorological 16-point roses. A wind from the north appears as a line toward the top of the page. Any wind between 348.75 and 11.24 degrees is considered to be a north wind, between 11.25 and 33.74 degrees, a north-northeast wind, and so on. The averaged insolation and temperature are shown for each hour.

The diurnal variation in wind direction is clearly evident at 10 and 61 m levels in the valley. The return circulation on the ridge is also shown, although much less apparent. This counter circulation appears mostly as southwest to southeast winds at night and as prevailing westerly winds during the day. A longer averaging period, say, for example, over the entire summer, would no doubt show the return circulation more clearly. However, since the length of daylight hours changes considerably at this latitude, it would be better to average the same month for a number of years rather than all the months for one year. Thirty-one days, however, were sufficient to produce meaningful results.

The difference in amplitude of the diurnal temperature variation is to be noted. The maximum averaged temperature differences during the day in degrees Celsius are 8.6, 7.5, 6.3, and 5.9 for the 10 m level (valley), 61 m level (valley), 10 m level (ridge), and 61 m level (ridge) locations, respectively. The temperature difference in these averaged peak-to-peak values between the valley and the ridge are 2.3° and 1.6 °C for the 10 m level (valley) minus the 10 m level (ridge), and the 61 m level (valley) minus the 61 m level (ridge), respectively. These numbers are averaged over the 31 days of August; individual days may be greater or less. It is this difference which causes the valley-plain breeze.

The pibal soundings show the counter current more clearly than the tower data. The counter current is often only directly above the center of the valley and, thus, not detectable with the tower measurements. The pibol soundings often show a low level jet near or slightly above ridge height. A low level jet is a local maxima in the wind speed, possibly accompanied by a directional shear within the boundary layer. It is believed that the low level jets apparent in the pibol records are a result of the counter current. When the prevailing winds are in the direction of the counter current, the local maxima appear higher in elevation than when they are opposing each other. A local minimum in the prevailing winds occurs at counter current height, thus producing a local maximum just below when the counter current and the prevailing winds are opposing each other. Similar maxima with a directional shear occur with crosswinds. The height and strength of the jet are a function of wind direction. Figure 8 shows typical wind profiles illustrating these maxima.

II. DATA ANALYSIS

A chronological synopsis of the local prevailing weather which occurred during the measurement program is presented in this section for the time periods October 1-5, 11-12, and 21-28. This is done on a 24-hour basis, 1700 to 1700 LST, corresponding to the time period shown in each figure. Airplane temperature soundings are superimposed at the same vertical scale as the acoustic record. Pibal readings are discussed with respect to the valley and counter valley flows. The sky

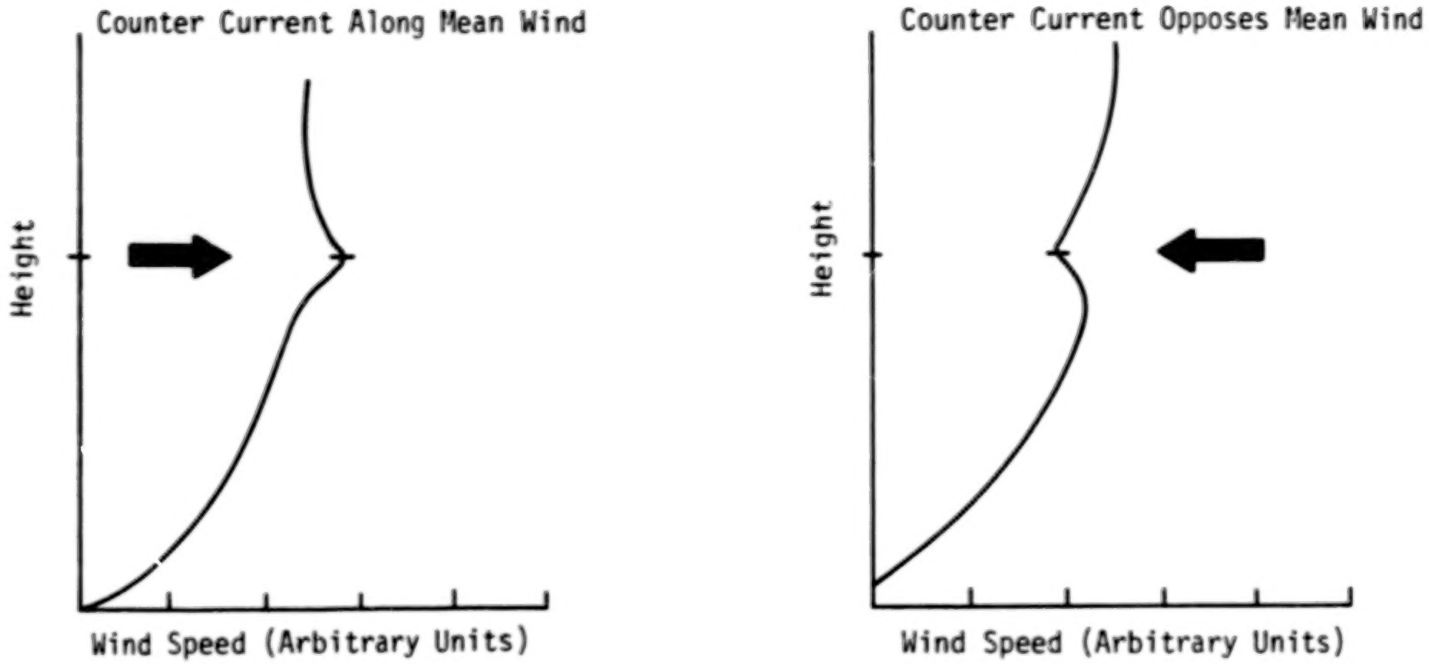

Figure 8. Arbitrary wind profiles illustrating the low level jet.

cover, barometric pressure, and prevailing winds are also reported along with the time of change in the direction of the wind.

Both acoustic radars were operated at the valley location during the time illustrated in Figures 9, 10, and 11. The purpose of locating the radars adjacent to each other was to compare the vertical axis of one radar with the other. The numerous dashed vertical lines appearing at approximately every five minutes are the result of slight differences in the height scale of the recorders. The transmitted acoustic pulse of one recorder appears on the record of the other recorder as a vertical line. Both the upper and lower charts on these figures appear nearly identical. One of the acoustic radars was moved to the ridge location on the afternoon of October 5, extreme right side of Figure 11.

October 1-2, Figure 9

By 1700 LST the sky had cleared from a stratocumulus deck which was prevalent earlier in the day. The down-valley breeze had set up by 1430 LST, which is earlier than normal. A temperature sounding at 2010 LST indicated the formation of an inversion at 500 meters which corresponds to the formation of the elevated inversion shown on both acoustic records. The acoustic records also show that a ground based inversion began to form shortly thereafter. A 1900 LST pibal reading showed northeasterly winds up to 1 km with a low-level maximum from the north at ridge height. This is a result of the minimum just above the jet due to the counter current. The evening remained clear and the pressure continued to rise steadily. Visual observation revealed that the plume which had been coning began fanning out beneath the 400 m inversion by 2200 LST.

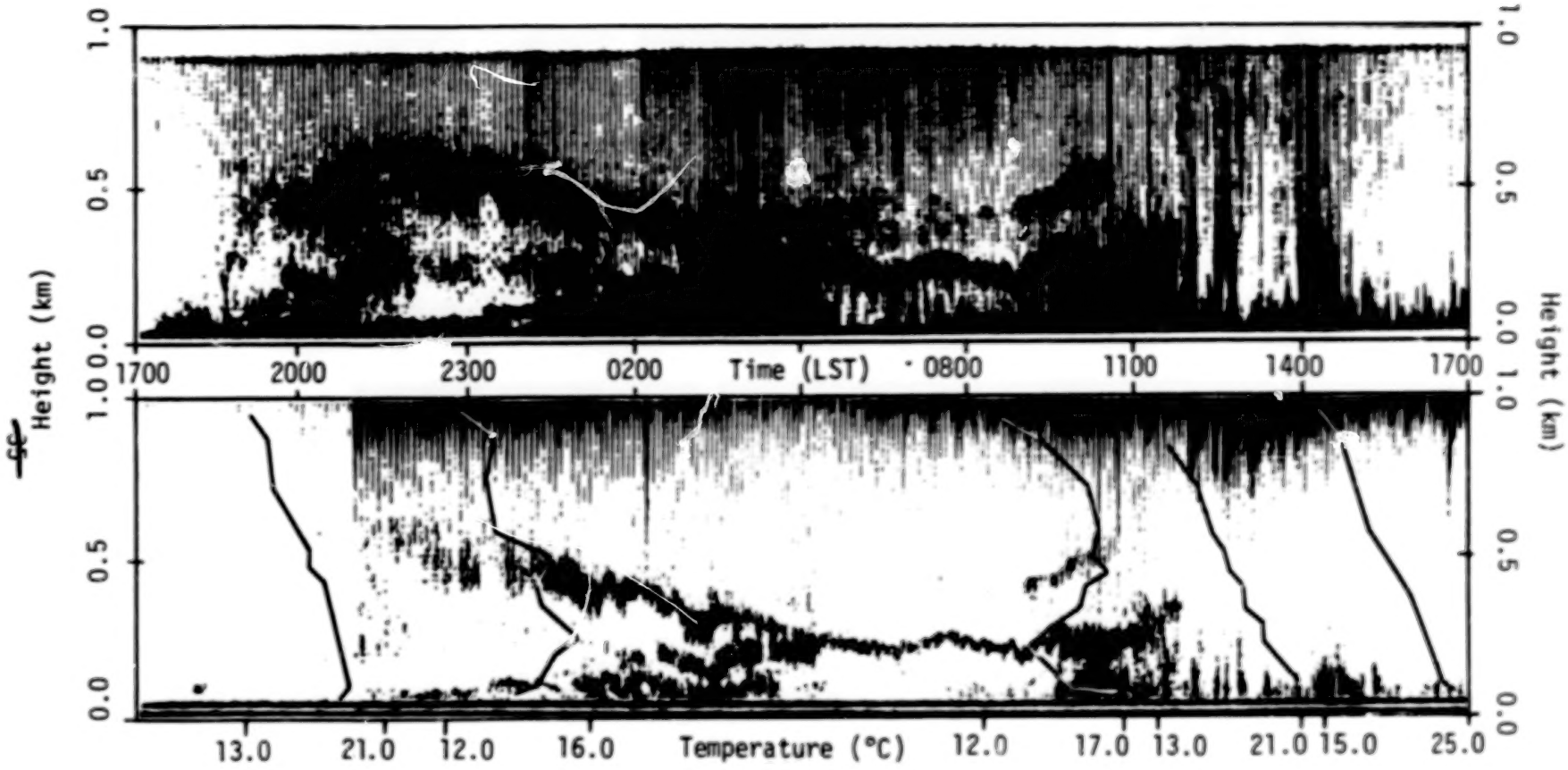

Figure 9. Acoustic records for Widows Creek steam plant (parallel operation, valley location), October 1-2, 1978.

BLANK PAGE

BLANK PAGE

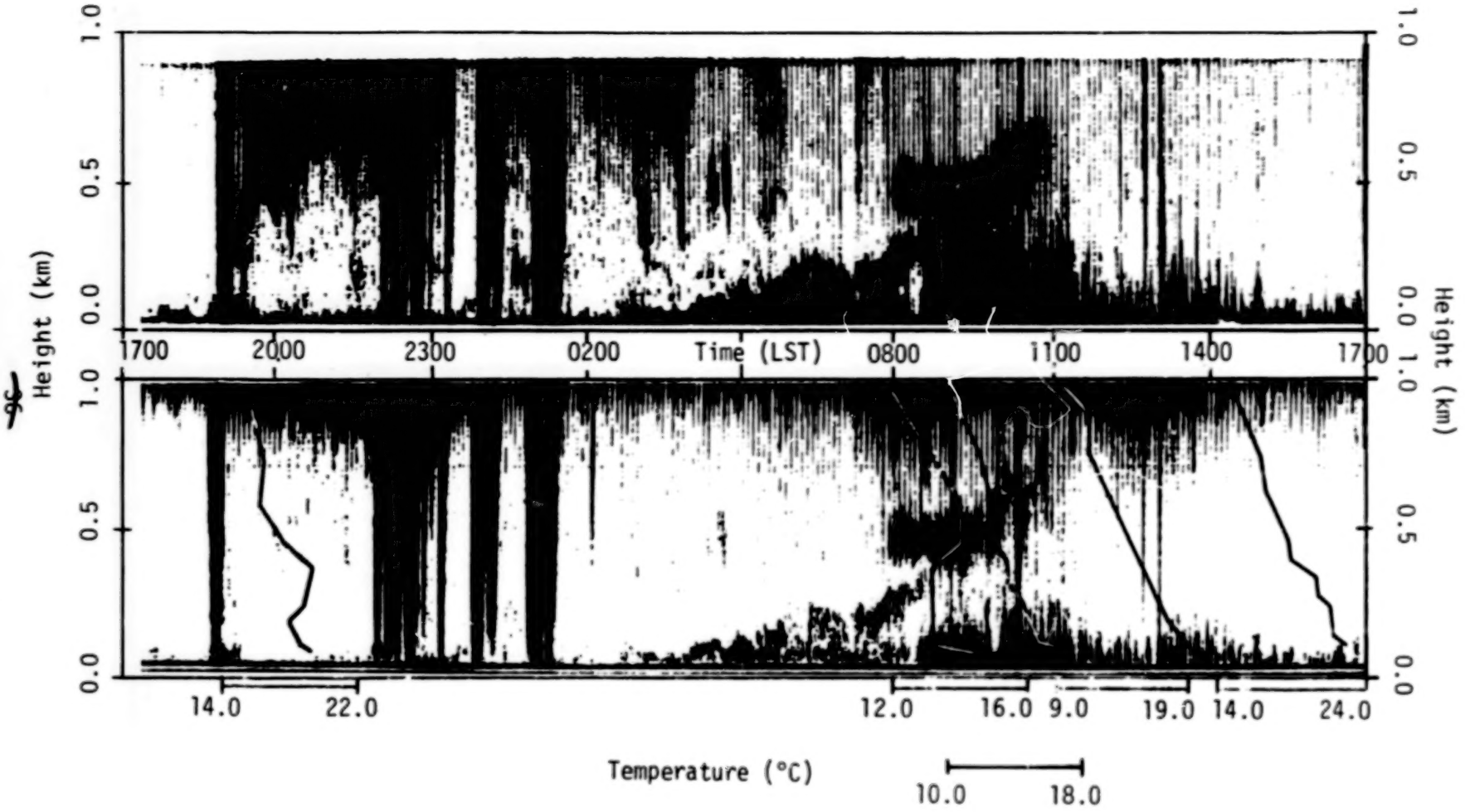

Figure 10. Acoustic records for Widows Creek steam plant (parallel operation, valley location), October 3-4, 1978.

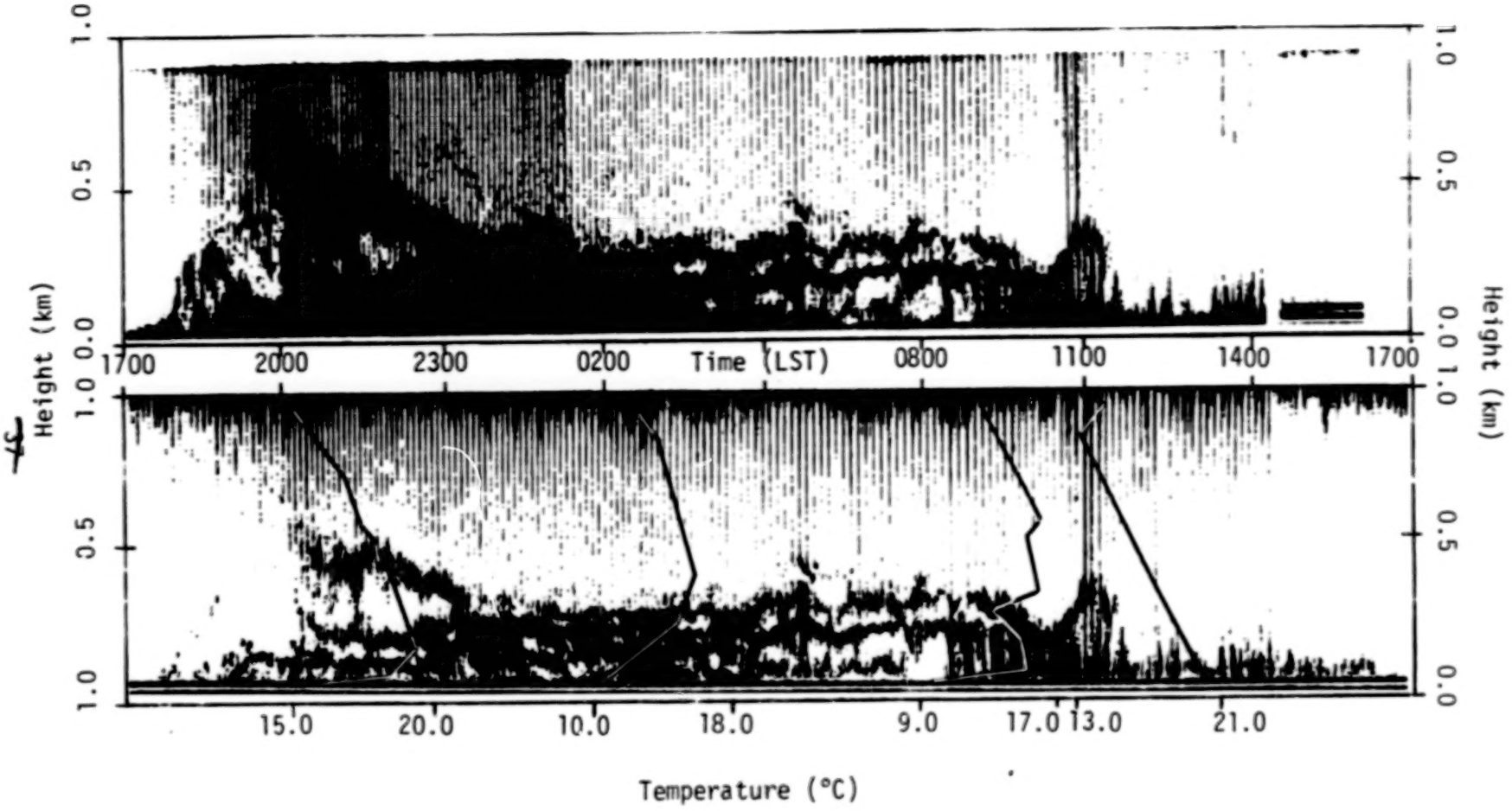

Figure 11. Acoustic records for Widows Creek steam plant (parallel operation, valley location), October 4-5, 1978.

The sky remained clear on the morning of October 2, and the pressure continued to rise. A temperature sounding at 0005 LST showed both a ground-based inversion and an elevated inversion of 400 m. Pibal readings at 0100 LST and 0300 LST showed a low-level jet at ridge height but very little change in direction from the prevailing winds which were still northeast up to a height of 1.5 km.

A thick fog had formed which obscured the sky by 0400 LST. A rawinsonde recording at 0430 LST showed only a ground based inversion up to 500 m. The fog remained thick until 1000 LST, after which time only patches of fog were left. A temperature sounding at 1010 LST showed two elevated inversions with the highest one being very weak. A 1015 LST pibal reading showed that the low level jet was weakening and had disappeared by 1202 LST.

The inversions had been eroded by thermals when the 1205 LST temperature sounding was made. The up-valley wind began to form by 1130 LST and continued to develop until 1700 LST. The sky was scattered with fair weather cumulus for the afternoon, and the pressure began to fall steadily from 1300 LST on. The time of decay of the jet and the formation of the up-valley wind corresponded perfectly.

October 3-4, Figure 10

On the evening of October 3, the up-valley winds continued exceptionally longer than normal, lasting well past 1900 LST. A stratocumulus deck had formed with a thin altocumulus deck above. A temperature sounding at 2010 LST shows the formation of an elevated inversion at 400 m. This is one of the few cases where the acoustic

record does not clearly show the inversion. Figure 10, upper chart, shows the inversion, but it is indistinguishable from the noise above it. The original facsimile recording of Figure 8, lower chart, shows a weak return, but it did not reproduce on this illustration. The 1900 LST pibal reading indicates that the low level jet at ridge height was from the southwest with no directional shear.

The broad vertical lines shown on the acoustic record are the result of a number of showers which passed over the area. The pressure began to rise and the prevailing wind, now northeasterly, formed a shallow fog by 0100 LST on October 4. A rawinsonde sounding at 0027 LST showed a positive lapse rate up to 2 km.

By 0400 LST the sky had cleared, and the pressure continued to rise. A rawinsonde sounding at 0413 LST showed that a shallow ground based inversion had formed up to 100 m. A 0640 LST pibal reading showed no evidence of a low-level jet in the strong prevailing winds which were northeast at the surface and veered to the west at a height of 1200 m.

The fog was quickly diminished due to surface heating after sunrise. An 0840 LST temperature sounding showed an inversion at 500 m, but the 1006 LST temperature sounding showed only an isothermal layer. A possible explanation for the apparently contradictory soundings may be that the strong echo at 550 m was formed by the plume or a warm bubble and that the 1066 LST sounding did not encounter the warm area.

Fair weather cumulus characterized the rest of the day. The 1215 LST temperature sounding showed an adiabatic lapse rate, and the acoustic record showed thermals until 1700 LST. The prevailing northeasterly winds apparently prevented the up-valley wind from forming.

October 4-5, Figure 11

The 1700 LST temperature sounding on October 4 continued to show an almost adiabatic lapse rate, and the acoustic record showed no returns. The sky remained clear, with the weak high pressure regime already becoming modified. The 1900 LST pibal reading indicated veering of the wind from northeast at the surface through the south to southwest at 1.5 km. A weak low-level jet began to form at ridge height. The 2035 LST temperature sounding shows the formation of a ground based inversion. The rest of this day remained clear and the jet at ridge height strengthened.

By 0302 LST on October 5, the ground based inversion is shown to have deepened to 400 m. A pibal reading at this time indicated that the wind veered to the southwest directly above the inversion top much lower than previously. A deepening fog formed by 0400 LST.

By 0700 LST the fog was almost 300 m deep. The temperature sounding at 0924 LST showed a strong shallow ground based inversion, a strong elevated inversion at 300 m, and a weak inversion at 600 m. The acoustic record does not show a return from 600 m.

By 1000 LST the synoptic wind was southerly at the surface, and the 1105 and 1300 LST pibals showed southwesterly to westerly winds up to 1.5 km with weak jets at ridge height due to the minimum at counter current height. A temperature sounding at 1224 LST showed a positive lapse rate to 1 km. The acoustic record showed only thermal echoes.

October 11-12, Figure 12

A broken stratocumulus deck occurred at 1.5 km on the evening of October 11, and a pibal reading at 2200 LST indicated the prevailing

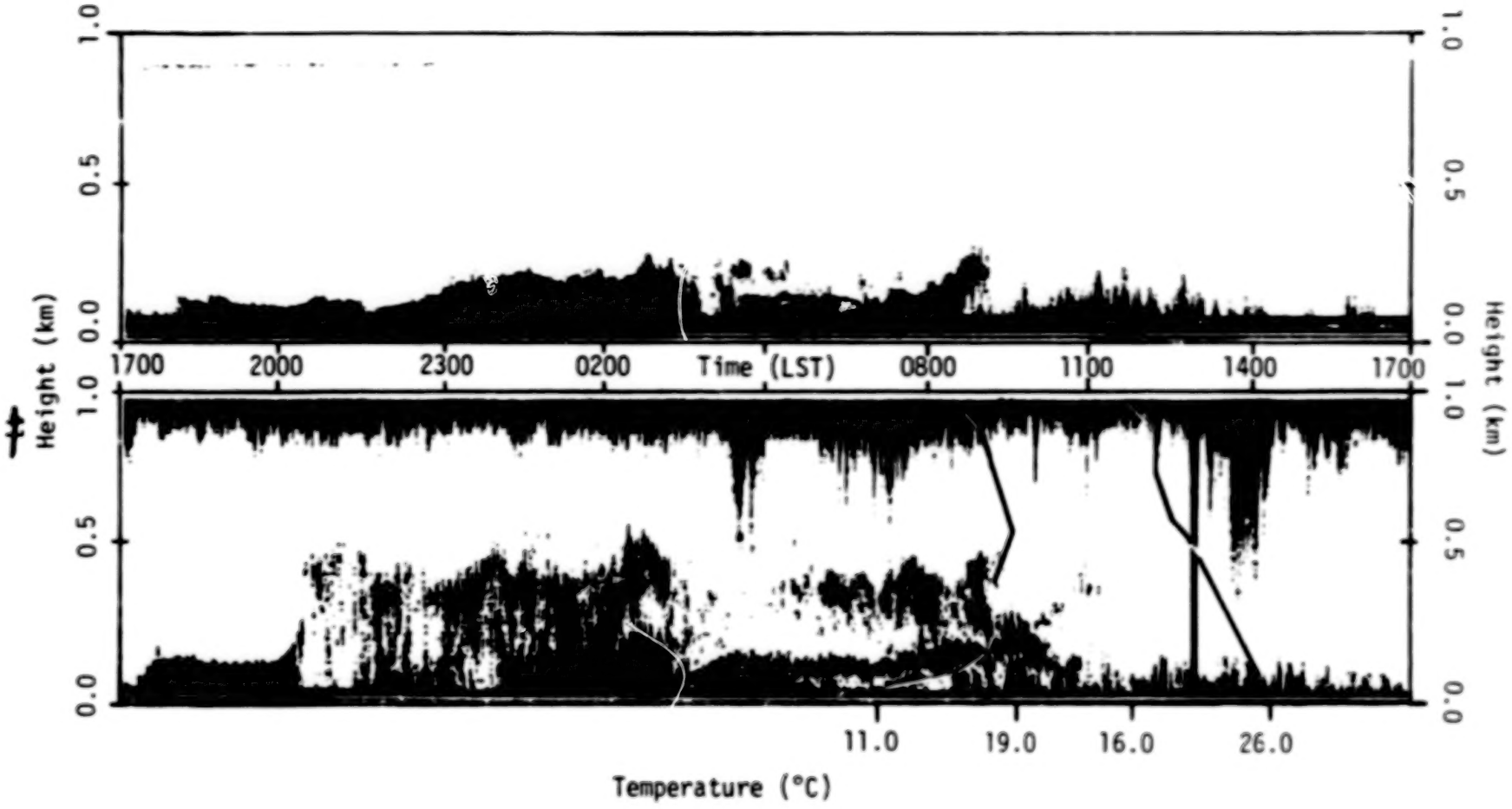

Figure 12. Acoustic records for Widows Creek steam plant, October 11-12, 1978. (a) Ridge location (upper chart). (b) Valley location (lower chart).

winds were southwesterly to a height of 1.5 km. A pibal reading at 2312 LST showed the formation of a jet at ridge height and the winds continuing from the south southwest to heights of 1.5 km. The acoustic record shows a deep ground based inversion, 400 to 500 m, in the valley and a shallow ground based inversion, 100 to 200 m, on the ridge. It should be noted that the difference in the heights of the inversion is nearly equal to the height of the ridge, approximately 300 m.

The sky had cleared by 0100 LST on October 12, and the down-valley wind finally set up over the strong southerly winds by 0300 LST. A pibal reading at 0305 LST showed a weak jet above the inversion top. By 0700 LST the sky was again covered with a stratocumulus cloud deck. A temperature sounding at 0844 LST showed a negative lapse rate up to 600 m. A pibal reading at 0700 LST showed the jet still existed and that the prevailing winds were south southeast to 1.5 km. By 1000 LST the cloud deck broke up, now covering only one-tenth of the sky, and the down-valley wind diminished. Pibal readings continued to show south-southwest winds up to 1.5 km with no apparent jet occurring. A temperature sounding at 1238 LST showed no inversion, while the acoustic record showed forming thermals. The inversion breakup on the plateau occurred almost two hours earlier than in the valley. The periodic black vertical lines caused by a lawn mower at 1400 LST are shown on the acoustic record from the valley.

October 21-22, Figure 13

A strong high pressure regime had moved into the area with clear skies. The down-valley breeze began to set up by 1900 LST and by 2000 LST was evident at 61 m. A temperature sounding at 2011 LST indicated

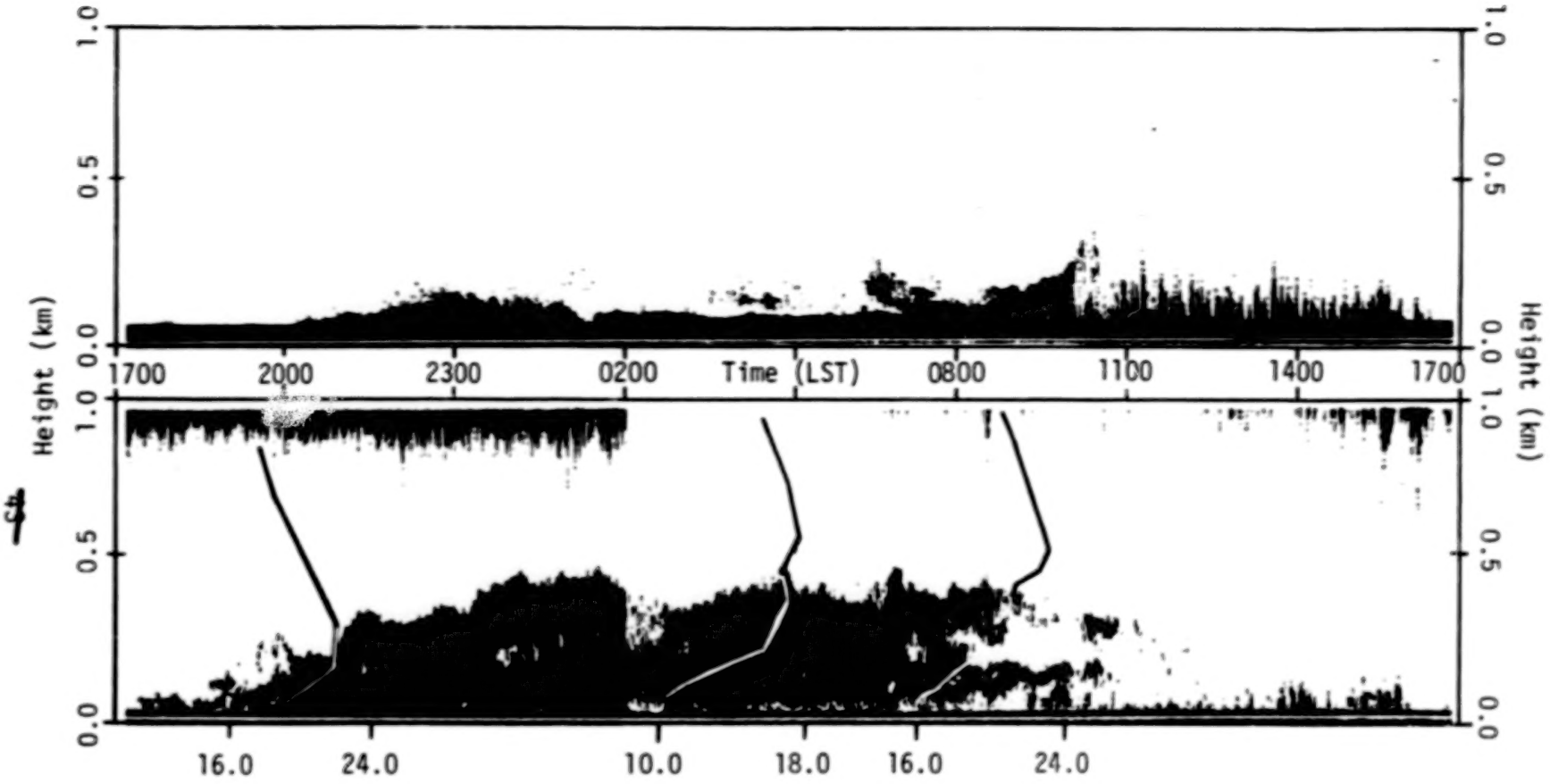

Figure 13. Acoustic records for Widows Creek steam plant, October 21-22, 1978. (a) Ridge location (upper chart). (b) Valley location (lower chart).

the formation of a ground based inversion up to 300 m. A pibal reading at 2315 LST showed southerly winds up to 1.5 km starting just above the down-valley breeze with a jet at ridge height.

The plume was fanning out beneath the inversion and creating higher than normal SO_2 concentrations at the surface early on October 22. The sky remained clear, and pibal readings at 0220 LST and 0500 LST continued to show southerly winds above 76 m, with northerly winds below this level and the appropriate jet. A temperature sounding at 0400 LST indicates a strong, deep ground based inversion up to 500 m. Again, the extremely shallow inversion on the ridge is to be noted.

The sky remained clear and the plume continued to fan out beneath the inversion, creating some SO_2 readings at the surface. A pibal reading at 0710 LST continued to show southerly winds, the down-valley breeze had deepened to 200 m, and the jet weakened. A temperature sounding at 0820 LST showed little change from that at 0400 LST. A cirrus deck began to invade the sky by 1000 LST and by 1300 LST covered the whole sky. The up-valley winds had formed at the surface by 1100 LST and moved upward to 61 m by 1200 LST. Pibal readings at 1109 LST and 1330 LST showed southerly winds up to 1.5 km with no jets. A temperature sounding at 1210 LST showed a positive lapse rate, while the acoustic record showed growing thermals. The much quicker and earlier breakup of the inversion on the ridge is again to be noted. The decay of the jets is the result of the change in counter current direction.

October 23-24, Figure 14

The clear high pressure regime remained in the area through October 24. The down-valley breeze had set up by 1700 LST. A pibal reading at 2220 LST showed northwesterly wind veering to westerly at 1 km with a jet occurring at ridge height. A pibal reading at 2330 LST showed northwesterly winds up to 1.5 km.

A low cumulus deck began to form early on October 24. A rawinsonde record at 0014 LST showed the formation of a weak elevated inversion at 800 m. A pibal reading was attempted at 0300 LST, but was lost at 300 meters because the sky was by now covered by clouds. A rawinsonde temperature sounding at 0357 LST showed a strong inversion topping out at 1 km. The acoustic record shows the height of a fluctuating inversion between 300 and 600 m over the ridge and between 700 m to off-the-chart in the valley.

Pibals reading at 0630, 0800, 0900, 1000, and 1100 LST were all lost in the clouds, a height too low to be of any significant value. Airplane temperature soundings were aborted due to the low-level clouds below inversion height at 0820 and 1000 LST but did indicate superadiabatic lapse rates to 500 m. The plume was observed to be trapped below the strong inversion and descended to the surface a number of times. A pibalreading at 1155 LST showed northeast winds below the inversion, with southwest winds above. A temperature sounding at 1215 LST located the inversion near 800 m.

The sky cleared by 1300 LST and remained clear until late afternoon on October 25. A pibal reading at 1300 LST continued to show strong shear just above inversion height. A temperature sounding at 1615 LST

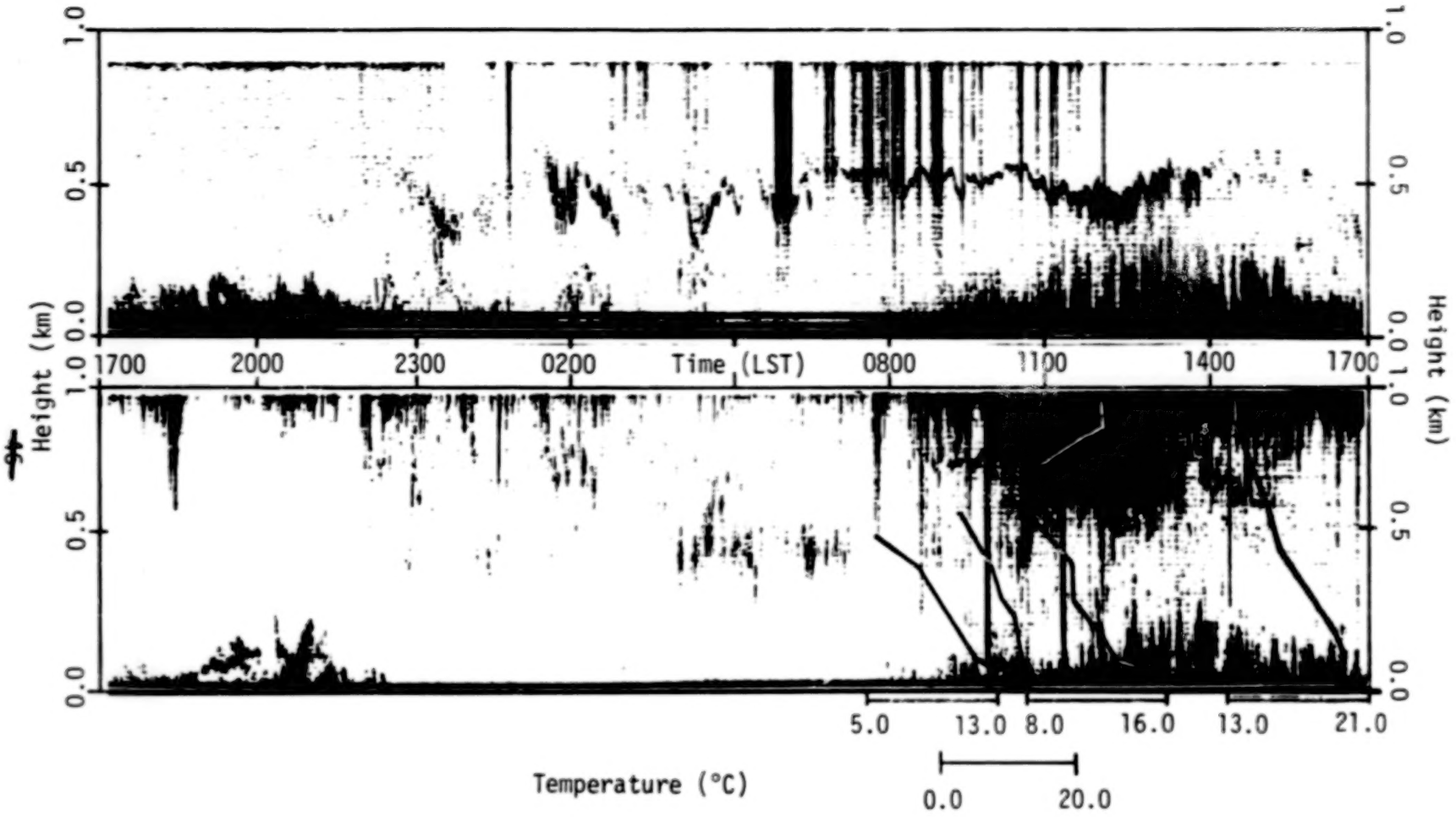

Figure 14. Acoustic records for Widows Creek steam plant, October 23-24, 1978. (a) Ridge location (upper chart). (b) Valley location (lower chart).

showed only an isothermal layer between 900 and 100 m, accounting for the weak echoes still shown on the acoustic record.

October 25-26, Figure 3(a), Page 14

The afternoon of October 25 was hazy and totally overcast with a cover of clouds between 1.5 and 2.0 km. Moderate winds were from the southeast at the surface and were southwest up to 1.5 km. The 1839 LST pibal reading showed moderate wind shear at 300 m, which corresponds well with the height of the forming ground based inversion. The sky cleared and the inversion top was near 600 m by 2000 LST. The haze continued and thin clouds formed again early on October 26. The aircraft soundings flown at 0300 and 0640 LST show the ground-based inversion top near 700 m. This is clearly shown on the acoustic record with the "quiet" area in between corresponding to the positive lapse rate shown in the soundings between 600 and 800 m. By 0640 LST the lowest inversion was no longer ground based and lowered to 500 m.

The down-slope winds did not set up until 0230 LST and lasted only until 0400 LST. The drainage wind was extremely weak and the prevailing southwesterly wind was observed at 61 m. The wind returned to the southwest at 0400 LST, and the surface warmed, destroying the ground-based inversion at 0600 LST. This registered on both the acoustic record and temperature soundings.

At 0600 LST the drainage wind set up, again only at the surface. This produced a very shallow fog, and the sky was still visible. By 0800 LST the southwest winds returned and the 0815 LST sounding showed only a weak inversion at 500 m. The temperature sounding at 1000 LST

showed only an isothermal layer and by 1200 LST, only an isothermal layer at 900 m. The 1625 LST temperature sounding showed a positive lapse rate for the complete sounding. The acoustic record shows the afternoon thermals breaking through the inversion around 1200 LST. Pibal readings showed basically strong southwest winds reaching a maximum of 20 m s^{-1}. It is easy to understand why the valley and counter circulations are nonexistent with such strong prevailing winds.

October 26-27, Figure 3(b), Page 14

The prevailing southwesterly winds continued until 1900 LST, and the sky was completely overcast with a stratus deck near 1.5 km. The prevailing winds then veered from the west to northwest by 2100 LST, and the pressure began to rise moderately. The 2100 LST rawinsonde reading showed an inversion forming at 500 m.

The cloud deck had lowered to 1 km by 0100 LST on October 27, and the prevailing winds had shifted to the north to northeast by 0200 LST. The 0225 LST rawinsonde shows that the inversion at 500 m had strengthened and a negative lapse rate existed from 550 to 850 m.

The sky had cleared by 0400 LST, and a strong wind shear existed just above inversion height as the wind veered from the northeast to the west. The strong subsidence inversion associated with the oncoming high pressure, which reached 1020 mb by 0700 LST, is shown weakening and decaying in the four airplane soundings. A pibal reading at 1030 LST clearly shows the return circulation with a southerly wind at 630 m forming against the prevailing northerly winds. The inversion is totally broken down by 1450 LST. The plume from the power plant was observed to be trapped below the inversion until 1300 LST and a number

of times reached the surface, accounting for the high SO_2 concentrations downwind. The pibal readings indicated that the strong counterclockwise veering just above inversion height continued until 1400 LST.

At 1400 LST the up-slope winds formed in the valley, and weak thermals broke through the inversion. The up-slope winds did not last long and by 1630 LST the stronger northwesterly winds prevailed.

October 27-28, Figure 3(c), Page 15

The evening of October 27 remained clear with an almost adiabatic lapse rate at 1700 LST. The 1732 LST and 1900 LST pibal readings showed the wind direction veered with height from the northwest at the surface and north at ridge height, east at 1 km and southwest at 1.5 km. The temperature sounding at 2020 LST showed the formation of an inversion just above ridge height. The plume became trapped below the sinking inversion and by 2400 LST was below ridge height.

The temperature sounding at 0010 LST on October 28 shows a surface inversion rising to meet the sinking inversion which was at ridge height. By 0100 LST the inversions met and formed a single ground-based inversion; the 0225, 0426, and 0816 LST soundings showed only a ground-based inversion. The plume, being trapped below the ridge height until 0700 LST, fanned out just above ridge height until 0900 LST. At approximately 0900 LST the ground-based inversion again split. This is clearly indicated by both the acoustic record and the 0957 LST temperature sounding.

Pibal readings at 0300, 0550, 0700, 0752, 1000, 1055, and 1700 LST all show the low-level jet indicative of the return circulation pattern.

By 1220 LST the inversion was broken down and only thermal plumes appeared on the acoustic record. The up-slope winds occurred only at the lowest level from 1500 to 1700 LST before the northerly winds again prevailed.

Discussion

One of the most persistent air pollution problems is created by the subsidence inversion. The inversions formed by the diurnal effect of mesoscale climates associated with mountain-valley systems can be as serious. Subsidence inversions occurred during the periods shown in Figures 3(b), 3(c), 9, and 14, pages 14, 15, 35, and 46. Higher than normal SO_2 concentrations were recorded downwind on three of the four days shown. The SO_2 concentration data were missing for October 1-2, Figure 9. Deep ground-based inversions occurred in the valley during the times shown in Figures 3(a), 11 through 13, pages 14, 37, 41, and 43. Higher than normal concentrations of SO_2 were recorded on three of the four days shown. During October 4-5, Figure 9, there were only occasional times when the SO_2 concentrations were measurable.

The ground-based inversions shown in Figures 12 and 14 are deep only in the valley. The effluent from a stack located on the ridge would not have been trapped below the inversions, as was the case in the valley. Ground-based inversions occur regularly on clear, calm nights. These inversions tend to extend just over the top of the ridge. The use of taller stacks, similar to the one at Widows Creek, which extend above the ridge will help to eliminate air pollution problems in the valley during these nocturnal conditions.

The use of larger stacks during periods when subsidence inversions exist will be of less value than for ground based inversions. The subsidence inversion shown in Figure 12, page 41, is at times 900 m above the valley floor. It would take an extremely large stack to insure no trapping of the plume below a strong inversion at this height.

CHAPTER IV

CONCLUSIONS

It is evident from the data presented here that the acoustic radar is as accurate in locating inversion levels as conventional rawinsonde or airplane soundings. Moreover, the acoustic radar has the advantage of continuously monitoring the inversion layers as opposed to periodic temperature soundings. The monostatic acoustic radar, however, does not give the magnitude of the temperature measurements, but only locates the spatial position of temperature discontinuities.

Calibration for quantitative analysis requires profiles of both temperature and the turbulence parameters. The aircraft was not equipped to measure turbulence, and therefore quantitative calibration was not attempted. Operation of two identical model radars side-by-side allowed for calibration of the height scales, but only visual calibration of the sensitivities. This, however, was sufficient for qualitative monitoring of the inversion layers. A monostatic acoustic radar, thus, provides an inexpensive means for continuous monitoring of inversions.

The difference in the structure of the atmosphere within and outside a large valley has been demonstrated. The acoustic record shows that the height of the major inversion is greater in the valley than on the ridge. The difference in height is approximately the height of the ridge. The use of taller stacks in the valley will be of greater value during times when ground-based inversions occur than when subsidence inversions occur.

BIBLIOGRAPHY

BIBLIOGRAPHY

1. Brown, E. H., and F. F. Hall, Jr. "Advances in Atmospheric Acoustics," Review of Geophysics and Space Physics, 16(No. 1): 47-110, February, 1978.

2. Kleppe, J. A., and H. L. Dunsmore. "Digital Signal Processing of Acoustic Radar Amplitude and Doppler Data," Proceedings of the Fourth Symposium on Turbulence, Diffusion, and Air Pollution. Boston: American Meteorological Society, 1979. Pp. 549-554.

3. Monin, H. S., and A. M. Yaglom. Statistical Fluid Mechanics. Vol. 2. Cambridge: The M. I. T. Press, 1975.

4. Tatarski, V. I. Wave Propagation in a Turbulent Medium. New York: Dover Publications, 1967.

5. Tatarski, V. I. "The Effects of the Turbulent Atmosphere on Wave Propagation." United States Department of Commerce, and National Science Foundation, 1971. Pp. 153-165.

6. Neff, W. D. "Quantitative Evaluation of Acoustic Echoes from the Planetary Boundary Layer." United States Department of Commerce National Oceanic and Atmospheric Administration, and Environmental Research Laboratories Technical Report, Boulder, Colorado, 1975.

7. Prandtl, L. Führer durch die Strömungslehre. Braunschweig, Germany: F. Vieweg and Sohn, 1942. Pp. 373-375.

8. Defant, F. "Local Winds," Compendium of Meteorology. Boston: American Meteorological Society, 1951. P. 665.

1. REPORT NO.	2. GOVERNMENT ACCESSION NO.	3. RECIPIENT'S CATALOG NO.
NASA CR-3401		

4. TITLE AND SUBTITLE	5. REPORT DATE
Analysis of the Inversion Monitoring Capabilities of a Monostatic Acoustic Radar in Complex Terrain	April 1981
	6. PERFORMING ORGANIZATION CODE
7. AUTHOR(S)	8. PERFORMING ORGANIZATION REPORT #
David Koepf and Walter Frost	
9. PERFORMING ORGANIZATION NAME AND ADDRESS	10. WORK UNIT NO.
Atmospheric Science Division The University of Tennessee Space Institute Tullahoma, Tennessee 37388	M-344
	11. CONTRACT OR GRANT NO.
	NAS8-32031
12. SPONSORING AGENCY NAME AND ADDRESS	13. TYPE OF REPORT & PERIOD COVERED
National Aeronautics and Space Administration Washington, D.C. 20546	Contractor Report (Final Report)
	14. SPONSORING AGENCY CODE

15. SUPPLEMENTARY NOTES **Technical monitor: O. H. Vaughan, Jr.**

Prepared under the technical monitorship of the Atmospheric Sciences Division, Space Sciences Laboratory, NASA, Marshall Space Flight Center, Alabama

16. ABSTRACT

A qualitative interpretation of the records from a monostatic acoustic radar is presented. This is achieved with the aid of airplane, helicopter, and rawinsonde temperature soundings. The diurnal structure of a mountain-valley circulation pattern is studied with the use of two acoustic radars, one located in the valley and one on the downwind ridge. The monostatic acoustic radar was found to be sufficiently accurate in locating the heights of the inversions and the mixed layer depth to warrant use by industry even in complex terrain.

17. KEY WORDS	18. DISTRIBUTION STATEMENT
Acoustic radar Complex terrain measurements Inversion measurements	Unclassified - Unlimited Subject Category 47

19. SECURITY CLASSIF. (of this report)	20. SECURITY CLASSIF. (of this page)	21. NO. OF PAGES	22. PRICE
Unclassified	Unclassified	59	A04

For sale by National Technical Information Service, Springfield, Virginia 22161

NASA-Langley, 1981

END

June 17, 1981